Ion-Molecule Reactions and Collision-Activated Dissociation of $C_4H_4^{+\cdot}$ Isomers: A Case Study in the Use of the MS^3 Capabilities of a Pentaquadrupole Mass Spectrometer

Brian J. Shay, Marcos N. Eberlin,* and R. Graham Cooks

Department of Chemistry, Purdue University, West Lafayette, Indiana, USA

Chrysostomos Wesdemiotis

Department of Chemistry, University of Akron, Akron, Ohio, USA

Isomeric $C_4H_4^{+\cdot}$ radical cations vinylacetylene (a), butatriene (b), methylene cyclopropene (c), and the nonaromatic cyclobutadiene (d), generated, respectively, from the neutral precursors 3-butyn-1-ol (1), 1,4-dichloro-2-butyne (2), benzene (3), and 7,8-benzotriciclo [4.2.0^{2,5}]deca-3,7,9-triene (4), undergo diagnostically different ion-molecule reactions with allene, isoprene, furan, and thiophene. It is speculated that adducts are generated by [2 + 2] cycloadditions with the first reagent and [4 + 2] Diels-Alder cycloadditions with isoprene, furan, and thiophene. The initially formed cycloaddition adducts fragment rapidly, isomerize, or undergo further addition of neutral reagent to yield a complex set of products. With a pentaquadrupole mass spectrometer, MS^3 experiments that employ three stages of ion mass analysis are used to help elucidate the ion-molecule reactions and to distinguish the isomeric $C_4H_4^+$ ions. Among these experiments, the reaction intermediate spectrum reveals the nature of the intermediates connecting the reactant to a selected product while the sequential product spectrum provides mechanistic and structural information on the adducts and other ion-molecule products. The unique combination of ion-molecule reactions with collision-activated dissociation employed here provides valuable information on the chemistry of ionized cyclobutadiene, including its proclivity to undergo [2 + 2] and [4 + 2] cycloadditions. (*J Am Soc Mass Spectrom 1992, 3, 518–534*)

It has long been recognized that ion-molecule reactions in the gas phase are particularly useful for both exploring the intrinsic chemistry of isolated molecules and ions and diagnosing unknown ion structures [1]. Several important properties of isolated species, such as proton affinities of gaseous molecules [2] or nucleophilic reactivities of unsolvated anions [3], have been established through ion-molecule reactions. Moreover, recent studies show that individual substructures in polyfunctional ions can be identified with high specificity based on the products of ion-molecule reactions [4]. For example, the characterization of a set of highly functionalized terpenoids with neutral ethyl vinyl ether takes advantage of the fact that a vinyl addition product is observed for compounds containing the β-hydroxy carbonyl functionality [4a]. The most common method used for the characterization of ions is collision-activated dissociation (CAD). In certain cases, however, this technique cannot differentiate isomeric ions because their fragmentation is preceded by isomerization. In a few of these cases, ion-molecule reactions have been shown to minimize isomerizations that can complicate structural studies. For example, ion-molecule reactions with ethyl vinyl ether are successful in distinguishing ionized cyclohexene oxide from cyclohexanone in contrast to the identical behavior due to isomerization seen in CAD spectra of these ions [4b]. Similarly, $C_2H_5O^+$ isomers have been distinguished based on differences in their reactivities with NH_3[4a], buta-1,3 diene, and benzene [4d, 4e], and several $C_2H_3O^+$ and $C_2H_3S^+$ ions are distinguished by ion-molecule reactions with isoprene and with methylanisoles but are indistinguishable upon CAD [4j]. Ion-molecule reactions have also been used to derivitize, prior to CAD, ions with high isomerization proclivities [5a].
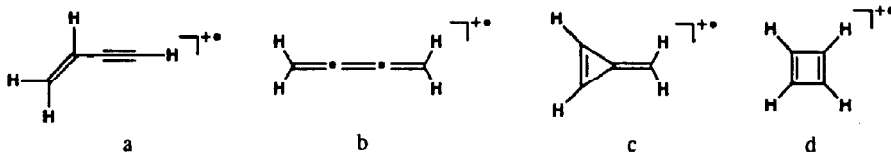
For example, the CAD spectra of $C_3H_5^+$ isomers show only a few minor differences, but those of their adducts with benzene are substantially different, thus allowing quantitative analysis of the $C_3H_5^+$ structures generated from various precursors [5b].

Gas-phase reactivity and structure characterization studies using ion-molecule reactions have employed many types of mass spectrometers [1f, 1g, 2, 3]. This article shows that such investigations are uniquely facilitated when using the pentaquadrupole mass spectrometer [6], which contains two separate reaction regions, each available for either ion-molecule reactions or CAD. Given the ability to mass-analyze ions before and after each of these regions with independent mass analyzers, a powerful set of MS^3 capabilities is provided [7]. These experiments allow access to specific types of information with significant advantages in chemical selectivity and speed of acquisition of data. MS^3 scans have also been implemented using three- and four-sector as well as hybrid instruments [8–10], although low energy ion-molecule reactions are difficult to perform with the former [11], and the pentaquadrupole is more versatile than the latter. Prior work has demonstrated the potential of MS^3 scans [7], including their ability to elucidate fragmentation patterns of octanones and to provide structural information on adduct ions, poly-isocyanates, and peptides [12–15].

The $C_4H_4^+$ system has been under active investigation for two decades. The available evidence indicates that both linear (a, b) and cyclic (c, d) forms are generated from ionized C_4H_4 neutrals or as fragmentation products from larger molecular ions. Until recently, structural characterization of $C_4H_4^+$ isomers had proved particularly difficult, principally due to the fact that the internal energy deposited in order to produce structurally diagnostic fragmentations causes unintended isomerizations. The difficulty of structural assignment has increased interest in these simple odd-electron ions and has given them importance as a proving ground for new approaches to ion structural determination.

action kinetics of $C_4H_4^+$ with benzene [18] (and later acetylene [19]) provided support for the existence of both linear and cyclic ions, as first suggested by the thermochemical data. However, studies of metastable ions [17, 18b] and CAD [18b] by most investigators supported the conclusion that the structure of $C_4H_4^+$ is independent of the precursor and of the method of formation. [Our own CAD spectra at very low collision energy—near zero—have also proved inconclusive. All isomers display the same set of product ions at very similar abundances, e.g., for ion **d**: m/z 52 (100%), m/z 51 (16%), m/z 50 (14%), and m/z 26 (21%).] These unresolved issues led Bowers [19] to reexamine the CAD spectra, and this work proved successful in distinguishing linear from cyclic $C_4H_4^+$ structures by differences in the characteristic $C_2H_2^+/C_2H_3^+$ ion abundance ratios. This finding reopened the question of just how many isomeric structures might exist, and a more recent CAD study indicated that structure **c** and the theoretically important cyclobutadiene radical cation (**d**) could be formed from novel precursors [20]. Indeed, the derivitization of ions **a**, **c**, and **d** with NH_3 confirmed their existence as distinguishable $C_4H_4^+$ isomers [21].

Recent neutralization-reionization mass spectrometry (NRMS) experiments [22] have shown distinct spectra for $C_4H_4^+$ ions generated from various precursors. NRMS is a relatively new technique that has shown strength in addressing questions of ion and neutral structure [23]. In NRMS one seeks to neutralize an ion by charge exchange, without accompanying isomerization, and then to dissociate the corresponding neutral in a high energy collision process. As isomerization barriers for neutral molecules are typically large, structural integrity is more likely to be maintained in the neutral than in the corresponding ion. Reionization of the fragments then provides a mass spectrum that characterizes the original ion structure [23a, 23b]. The neutralization-reionization (NR) spectra of ions **a–d**, produced from vinyl acetylene, butatriene, 6,7-benzo-3-methylenetricyclo-[3.2.2.0^{2,4}]nona-6,8-diene, and 7,8-benzotricyclo-

a   b   c   d

Rosenstock et al. [16] performed some of the first ionization and appearance potential measurements on C_4H_4 systems and suggested the existence of both linear and cyclic structures of the radical cation. In other early work, Baer et al. [17] measured average kinetic energy releases of metastable $C_4H_4^+$ ions and also calculated fragmentation rates to characterize the dissociating ionic species suggested to be the methylene cyclopropene radical cation (**c**). Ion-molecule re-

[4.2.2.0^{2,5}]deca-3,7,9-triene, respectively, provided clear evidence that these four isomers represent distinct, stable $C_4H_4^+$ cations [22]. The four isomers were distinguished by structurally significant and reproducible differences in their NR spectra. A follow-up NRMS study by Zhang et al. [24] analyzed the composition of $C_4H_4^+$ ions formed upon electron ionization of a large variety of organic molecules. The vast majority of the precursors, including benzene, were

Table 1. Thermochemical data[a]

Neutral compound	Ionization energy (eV)	ΔH_f^o (neutral) (kJ/mol)	$\Delta H_f^o(C_4H_4^{+\cdot})$ (kJ/mol)
Vinylacetylene	9.58	305	1229
Butatriene	9.15	349	1232
Methylenecyclopropene	8.28[b,c]	410	1209
Cyclobutadiene	8.02[b,d,e]	464[f]	1238[b]
Allene	9.69	190.6	
Isoprene	8.84	75	
Furan	8.883	−34.8	
Thiophene	8.87	115.0	

[a] Ref 25 unless otherwise noted.
[b] See ref 22.
[c] Also 8.15 eV (adiabatic) [26].
[d] ΔH_f^o (neutral) = ΔH_f^o (ion) − IE.
[e] Also 8.10 eV; ref 27.
[f] Based on $\Delta H_f^o(c)$ and the theoretically calculated energy difference between c and d from ref 28.

found to yield a mixture of 68% c (the most stable structure; see Table 1) and ~ 32% a. Notable exceptions were 3-butyne-1-ol and 1,4-dibromo-2-butyne, which produce pure a and mainly b (56%, along with 44% d), respectively.

To apply for the first time to a significant problem in ion chemistry the MS^3 capabilities of the pentaquadrupole mass spectrometer, we systematically examined the ion-molecule reactions of the $C_4H_4^+$ isomers a–d with the unsaturated reagents allene, isoprene, furan, and thiophene. Dienes were chosen as the reaction partners because their gas-phase cycloaddition to radical cations has been studied extensively, particularly by Gross and co-workers, and the mechanisms of these reactions have been investigated [29]. Our major objectives are (1) to explore the bimolecular chemistry of such novel gaseous ions as the cyclobutadiene (nonaromatic) and methylene cyclopropene (aromatic) cations and (2) to probe the potential of ion-molecule reactions in the pentaquadrupole to differentiate a complex system of isomers that may readily equilibrate. Parallels may exist with Diels-Alder reactions of radical cations and protonated molecules in solution [30, 31] and those in the gas phase, and this possibility was also considered.

Experimental

All studies (MS/MS and MS^3) were performed using a custom-built pentaquadrupole mass spectrometer [6a] with three mass-analyzing quadrupoles (Q1, Q3, Q5), typically operated at unit mass resolution, and two collision quadrupoles (Q2, Q4). Samples were introduced at room temperature via a vapor inlet probe and ionized by electron ionization (EI) of nominal 70 eV electron energy and at a source temperature of approximately 200 °C.

The isomeric C_4H_4 radical cations a–d were gener-

ated from 3-butyn-1-ol (1), 1,4-dichloro-2-butyne (2), benzene (3), and 7,8-benzotricyclo[4.2.2.0^{2,6}]deca-3,7,9-triene (4), respectively [16, 19, 22, 24]. As mentioned above, 1 and 4 produce pure a and d, respectively, and 3 yields predominantly (> 2/3) c. Although 2 has not been used as a $C_4H_4^+$ precursor previously, it is expected to form mainly b. This was determined in a precursor ion scan (B^2/E) of the $C_4H_4^+$ ions from 2, measured with the EBE tandem mass spectrometer at the University of Akron, which reveals that the majority of $C_4H_4^+$ (90%) originates from [M−Cl]$^+$ and a minor fraction (10%) is formed directly from M$^+$. The stepwise chlorine elimination, $ClCH_2-C \equiv C-CH_2Cl^{+\cdot} \to ClCH_2 \equiv C -CH_2^+ \to CH_2 = C = C = CH_2^{+\cdot}$ most probably produces ion b. The direct Cl_2 loss must proceed after ionization at the triple bond, which would allow the two terminal Cl atoms to approach each other; this mechanism can yield b, but cyclization during Cl_2 loss could also lead to d.

Ion-molecule reactions were performed by mass selection of $C_4H_4^+$ ions (m/z 52) in quadrupole Q3, reaction in Q4 with a neutral gas, with the spectra of the products being recorded by scanning Q5. Quadrupoles Q1 and Q2 were operated as wide bandpass m/z filters in the radiofrequency (RF)-only mode to transmit all source ions to Q3. An alternative method employed mass selection of m/z 52 in Q1, reaction in Q2, and Q3 as the product mass analyzer, while operating Q4 and Q5 in the RF-only mode. When characterizing ion-molecule products by the sequential product scan (MS^3) (see Table 2, row i), Q1 was used to mass-select the precursor m/z 52 ion for reaction in Q2, with Q3 being used to mass-select a particular product ion for CAD in Q4. The final quadrupole Q5 was then scanned to yield the sequential product spectrum. These spectra were typically recorded using a nominally zero collision energy in

Table 2. Scan symbolism, nomenclature, and examples of MS^3 experiments

Symbol[a]	Scan Type[b]	Examples				
		Q1	Q2	Q3	Q4	Q5
(i) ● ⇒ ● → ○	Sequential product	(52)	Allene	(91)	Argon	○
(ii) ● → ● → ○	Sequential product	(52)	Cyclohexane	(52)	Allene	○
(iii) ● → ○ → ●	Reaction intermediate	(52)	Allene	○	Allene	(131)

[a] A filled circle represents a fixed (or selected) mass; an open circle, a variable (or scanned) mass. A dark arrow represents a defined (usually fixed) mass transition; a light arrow, a variable mass transition.

[b] For more details on this nomenclature, see refs 7 and 32.

Q2 and 10-eV collisions in Q4 so that ion-molecule reactions would be restricted to Q2 and CAD to Q4.

Nominal sample pressures were typically 4×10^{-6} torr, as monitored by the single ionization gauge located in the vacuum chamber. The neutral gases in the collision quadrupoles were typically present at nominal pressures of 7×10^{-5} torr. As the instrument is not differentially pumped, a slight amount of mixing of source and collision gases is expected, although the flow of gas out of the shrouded collision cells through the lens apertures minimizes the entrance of other gases into these regions. Reactions with all four neutral reagents were performed on several occasions under both low and high sample pressures (as measured by the sum of all pressures recorded using the ionization gauge) to check for cross-contamination with the neutrals introduced into the ion source. The product ion abundance ratios were very similar under all conditions, and no new peaks appeared in the spectra.

To maximize the cross sections of ion-molecule reactions, ion translational energies were kept low. The translational energy is determined primarily by the voltage difference between the point of origin, usually the ion source, and the collision quadrupole. The collision energies given simply reflect the dc voltages on the collision quadrupole. Energies that maximize exothermic ion-molecule reactions fall near zero eV. Although with a grounded source (as used here) a negative voltage is usually applied to the collision quadrupole in experiments with positive ions, it was noticed that a slight positive dc voltage, typically +2 V, often enhanced the yield of ion-molecule reaction products.

The spectra displaying the products of reactions of C₄H₄+· with allene were acquired on several occasions under conditions in which different lens potentials and pressures of background, sample, and reagent gas (allene) were used. They were found to be reproducible only to within approximately +15%. For this reason and to minimize mass discrimination effects known to occur in quadrupole instruments [33], all instrument parameters—specifically the ionization energy, lens voltages, quadrupole dc voltages, collision gas pressure, and sample gas pressure—were held constant for a given experiment while the complete set of ions was studied. When this was done, reproducibility in ion abundances was approximately ±5%.

The data were acquired under computer control as single slow scans using an in-house acquisition program [32]. The MS^2 scans were typically obtained in under 20 s, and the MS^3 scans were acquired in less than 2 min.

Compound **4** was available from earlier work in Fred W. McLafferty's laboratory [22] and was synthesized from benzobicyclo[2.2.2]octadiene by Barry K. Carpenter and others [34]. All other reagents were commercially available and used without further purification other than a single liquid N₂ freeze-thaw cycle.

Results and Discussion

Reactions with Allene

The reactions of C₄H₄+· with allene provide product spectra that allow distinction among three of the four isomers (Figure 1). Distinction between ions **a** and **c** is not accomplished (Figure 1a and 1c), although the high relative abundances of ions at m/z 67, 79, and 119 differentiate these from the other isomers. Butatriene radical cation (**b**) has the highest m/z 64 and 103 peak intensities relative to m/z 65 and 119 (Figure 1b). Cyclobutadiene radical cation (**d**) yields the lowest intensity of several ions, specifically, m/z 79 relative to m/z 65 and 91 (Figure 1d).

The contribution to these spectra due to reactions of the charge exchange product, ionized allene (m/z 40), with neutral allene must be assessed in order to decide whether differences in charge exchange cross sections or ion-molecule reactivities underlie the distinctions seen in Figure 1. To do this, the allene radical cation formed in the ion source was mass-selected and reacted with allene (Figure 2) under the same conditions as used to acquire the spectra shown in Figure 1. Peaks at the same masses are observed in Figures 1 and 2, but ion m/z 79 in Figure 2 is displayed as the most abundant product. The m/z 79 ion also is the major product of the reaction of the allene radical cation with its neutral counterpart at thermal energies in an ion cyclotron resonance (ICR) mass spectrometer [35], indicating that the qualitative product distribution from this self-condensation is not susceptible to severe kinetic or internal energy effects (see below). The m/z 91/79 (and also the m/z 131/79)
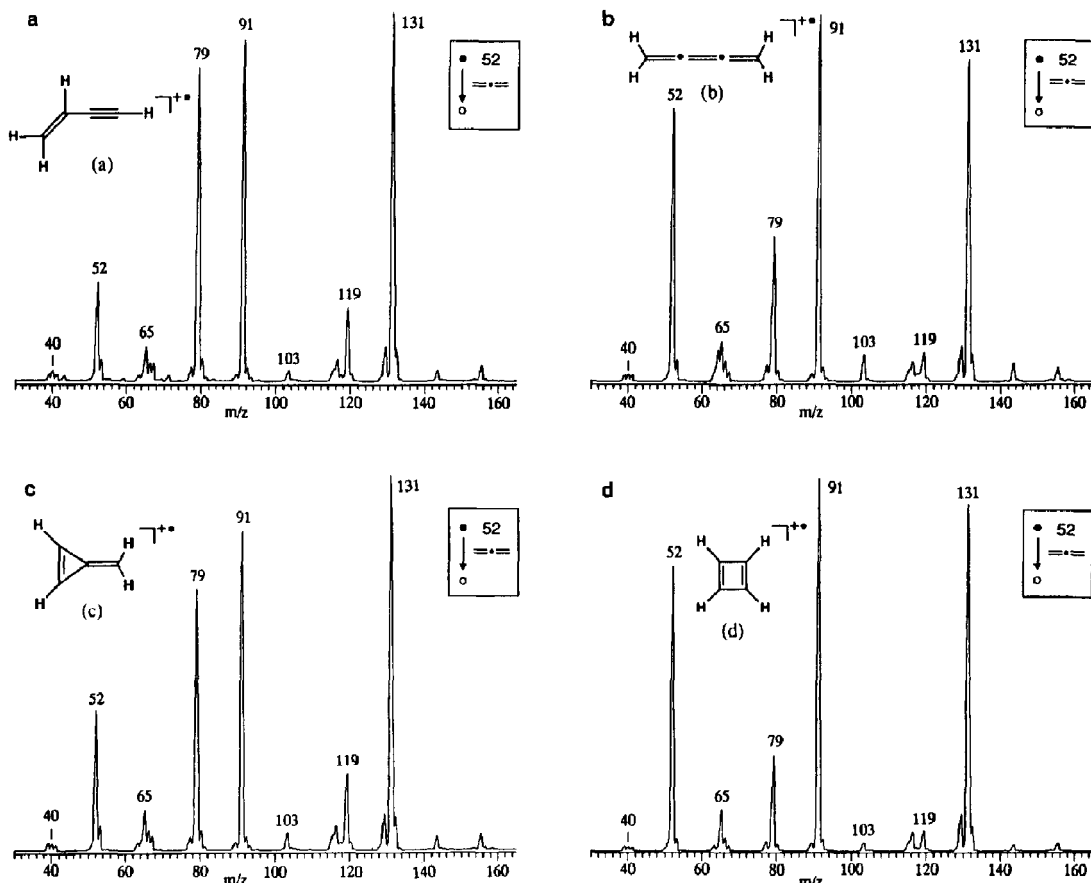
Figure 1. Product spectra of the ion-molecule reactions of ions **a-d** (m/z 52), respectively, with neutral allene showing [2 + 2] cycloaddition (m/z 91, 131), charge exchange (m/z 40), and other products.
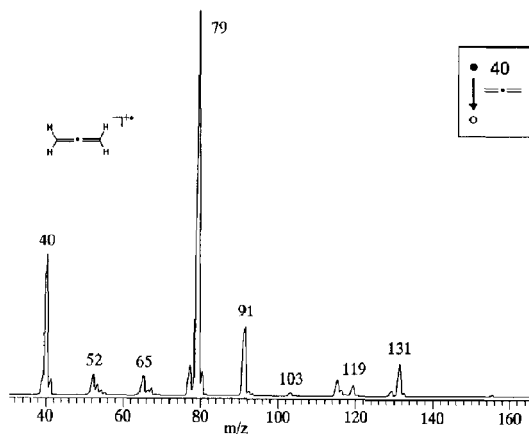

Figure 2. Product spectra of the ion-molecule reactions of the mass-selected allene radical cation (m/z 40) with neutral allene.

ratio in Figure 2 is much smaller than those observed in the $C_4H_4^{+\cdot}$ spectra (approximately one-twentieth that observed in Figure 1d); this indicates the minor role played by the charge exchange product, ionized allene, in the formation of m/z 91 and m/z 131, the smallest contribution of this process being observed for ion **d**. This minor role of the charge exchange channel is also substantiated below using reaction intermediate scans.

The ionization energy of allene is greater than the ionization energies of the neutrals corresponding to ions **a-d** (Table 2); therefore, change exchange with allene is endothermic for all four ions studied, with reaction enthalpies of approximately 0.1 eV for **a**, 0.5 eV for **b**, 1.4 eV for **c**, and 1.7 eV for **d**. The required energy is supplied from the translational energy of the ions. Based on the abundances of m/z 79 in Figure 1, the extent of charge exchange decreases from **a** to **b** to **d** as expected from the respective endothermicities. However, ion **c** exhibits a much larger preference for charge exchange than predicted

by the available thermochemical data. An issue also deserving attention in ion chemistry is the importance of the distinction of effects due to differences in internal energy from those due to structure [19, 36]. To evaluate this possibility, each of the four $C_4H_4^+$ ion populations formed from compounds 1-4 were generated using 16-, 20-, and 70-eV electron energies and reacted with allene. The resulting spectra (not shown) were very similar to the respective 70-eV spectra (major ion abundances were reproducible to approximately ±5%), which demonstrates the absence of significant internal energy effects. However, as discussed below, the vinylacetylene ion (a), when activated in a separate collision process prior to ion-molecule reaction with allene, showed a small but detectable dependence on internal energy. The behavior of ions a and b was also reported to be relatively independent of ion internal energy in ion-molecule reactions with benzene at various pressures [37]. In their CAD study of $C_4H_4^+$ ions Bowers and colleagues [19] and McLafferty and associates [22, 24] also indicate that significant internal energy effects are absent.

Reactions with Isoprene

These reactions yielded a distinctive spectrum for ion d, which shows relatively abundant reaction products at m/z 55, 77, 79, 91, 103, 105, and 173 (Figure 3a). The spectra for ions a, b, and c are all very similar; the spectrum of ion c is shown in Figure 3b. It is dominated by ions arising from charge exchange to form ionized isoprene (m/z 68), which subsequently reacts with isoprene neutrals to give m/z 67, 69, 81, 93, 94, 95, 107, 108, 121, 137, and 149. This pathway was confirmed by recording the spectrum (not shown) displaying the products of ion-molecule reactions between the isoprene radical cation (generated in the ion source) and isoprene neutrals.

Thorough kinetic and MS/MS studies by Gross and co-workers have demonstrated that cycloaddition and charge exchange are the predominant reactions between alkene radical cations and dienes (or vice versa) in the gas phase [29]. For the butadiene molecular ion–methyl vinyl ether pair it was shown that *exothermic* charge exchange is faster and therefore precedes the butadiene to methyl vinyl ether molecular ion cycloaddition [29a]. With isoprene as the diene, charge exchange is endothermic for c and d (0.6 eV and 0.7 eV; see Table 1) but exothermic for a and b (−0.7 eV and −0.3 eV). The reaction enthalpies can explain the significantly lower yield of charge exchange products from ion d in comparison to ions a and b but cannot justify the high efficiency of charge exchange with ion c. Apparently, nonthermochemical factors also influence the reaction outcome, as is indeed the case for cycloaddition in solution.

Pericyclic reactions with radical cations in the presence of an inert solvent have been studied extensively
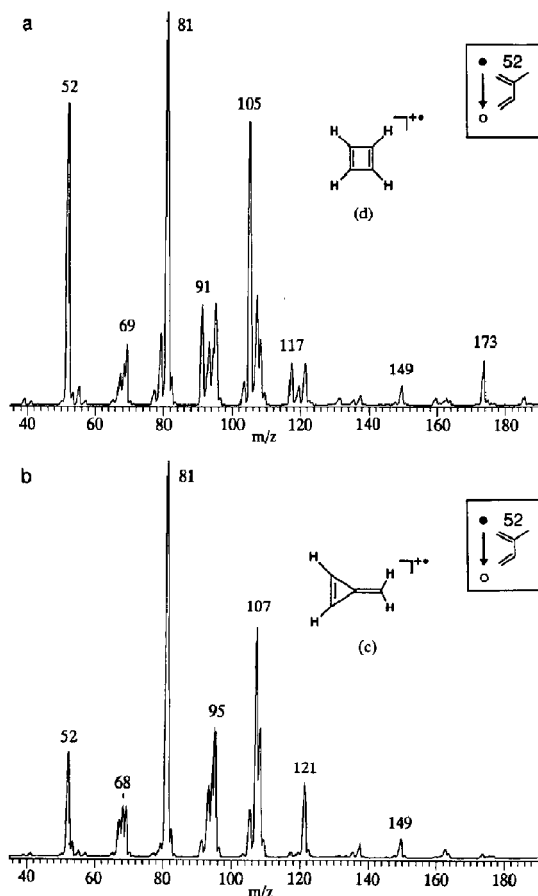

Figure 3. Product spectra of the ion-molecule reactions of (a) ion d and (b) ion c with neutral isoprene showing reaction products (m/z 91, 105, 117, 119, 173) for d as opposed to predominantly charge exchange products for c. Spectra for ions a and b are similar to the spectrum of c.

by Bauld and associates [31]. In solution the rates of such charge-catalyzed ("hole-catalyzed" according to Bauld) cycloadditions can be comparable to the rates of charge transfer between the dienophile radical cation-diene and independent of the thermochemistry of the latter process [31b]. Our present results agree with these findings. The profound differences in the reactivities of ions c and d most likely result from their fundamentally different structures: Ionization converts cyclobutadiene, an electron-rich diene, into an electron-poor, reactive dienophile that should undergo facile [4 + 2] cycloaddition with isoprene according to Bauld and colleagues [31].* As an allylic cation, ion d should also exhibit enhanced reactivity

---

* Bauld's studies predict [4 + 2] cycloaddition for the dienophile⁺/diene reaction but [2 + 2] cycloaddition for the diene⁺/dienophile [31b].

toward dienes based on Gassman's theory [30]. In such charge-catalyzed cycloadditions the electrophilic site of the dienophile (d) attacks the nucleophilic site of the diene (isoprene). In ionized methylene cyclopropene (c) the positive charge is delocalized in an aromatic ring, making ion c a much weaker electrophile and thus notably reducing its rate of cycloaddition to isoprene. A further reason for the lower reactivity of c versus d is that addition of isoprene removes aromaticity from c.

Reactions with Furan and Thiophene

Two heteroatom-containing compounds were also used as reagent gases to explore the reactions of $C_4H_4^+$ and to distinguish the isomers. Reacting each of the $C_4H_4^+$ ion populations with furan resulted in a spectrum that showed unique products for ion d, allowing differentiation from the other isomers. This spectrum (Figure 4a) shows high abundances of m/z 55, 81, 91, 105, 119, 131, and 159 ions (relative to the charge exchange peak at m/z 68, furan radical cation). The spectra for ions a–c are all similar, and each is dominated by the charge exchange product, m/z 68, and m/z 136, the furan dimer, as exemplified for ion b in Figure 5b, with $C_4H_4^+$ addition products contributing little to these spectra. The MS/MS product spectrum resulting when the furan molecular ion reacts with neutral furan shows m/z 136 as the only product and confirms the assignment of this ion as the furan dimer. The fact that the reactive diene, furan, like isoprene, forms a unique adduct only with ion d verifies the distinctive reactivity of this ion.

In ion-molecule reactions with thiophene, ion d is again very easily distinguished from the other isomers, and for the same reasons. Its spectrum (Figure 5a) displays little of the charge exchange product, the thiophene radical cation at m/z 84, but gives an abundant m/z 135 ion, and several medium to low abundance products at m/z 91, 97, 103, 110, 121, and 175 are present. Although ions a–c react predominantly by charge exchange (m/z 84) as observed previously in their reactions with isoprene and furan, ion a forms a unique stable adduct at m/z 136, which allows distinction of this ion (Figure 5b). Ion b yields a product spectrum very similar to that of ion c.

Although charge exchange dominates the behavior of ions a–c, the product, ionized thiophene (m/z 84), was shown not to undergo significant ion-molecule reactions with neutral thiophene by generating thiophene radical cations in the ion source and reacting them with the neutral in Q2. Ionized thiophene was shown to be much less reactive relative to furan in that no dimer was formed and higher neutral gas pressures were necessary to observe any products. The product spectrum displays the selected ion at m/z 84 (100%) and other products at m/z 98 (29%), 96 (54%), and 71 (15%). Of these ions only m/z 84
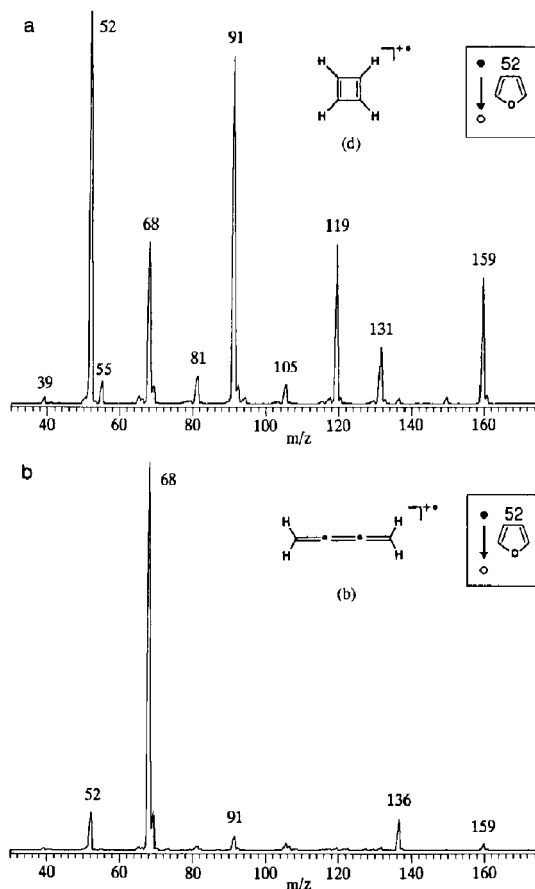

Figure 4. Product spectra of the ion-molecule reactions of (a) ion d and (b) ion b with neutral furan showing reaction products (m/z 81, 91, 105, 119, 131, 159) for d as opposed to primarily charge exchange products (m/z 68, 136) for b. Spectra for ion a and c are similar to the spectrum of b.

contributes significantly to the m/z 52 product spectra shown in Figure 5.

The characteristic [103+]:[119+] and [64+]:[65+] ion abundance ratios displayed for isomer b in Figure 1b as well as the [135+]:[136+] ratio for isomer a in Figure 5b show that isomer c is the major constituent of the $C_4H_4^+$ population detected for benzene (3) (Figures 1c and 5c) under the low energy collision conditions used here, in good agreement with recent NRMS studies [22, 24] proposing that the population of ions formed from 3 under 70 eV EI is a 32:68 mixture of a and c. Others have proposed ratios of $60:40 \pm 5$ (15 eV EI) [18a], $53:47 \pm 8\%$ (150 eV EI) [19], 0:100 (CI) [19], and more recently 60:30 with a 10% contribution from b [37]. As the distinction of isomer d is particularly clear in all four sets of ion-molecule product spectra, one can be confident in assigning a negligible contribution of this ion to the $C_4H_4^+$ population of precursors 1, 2, and 3.
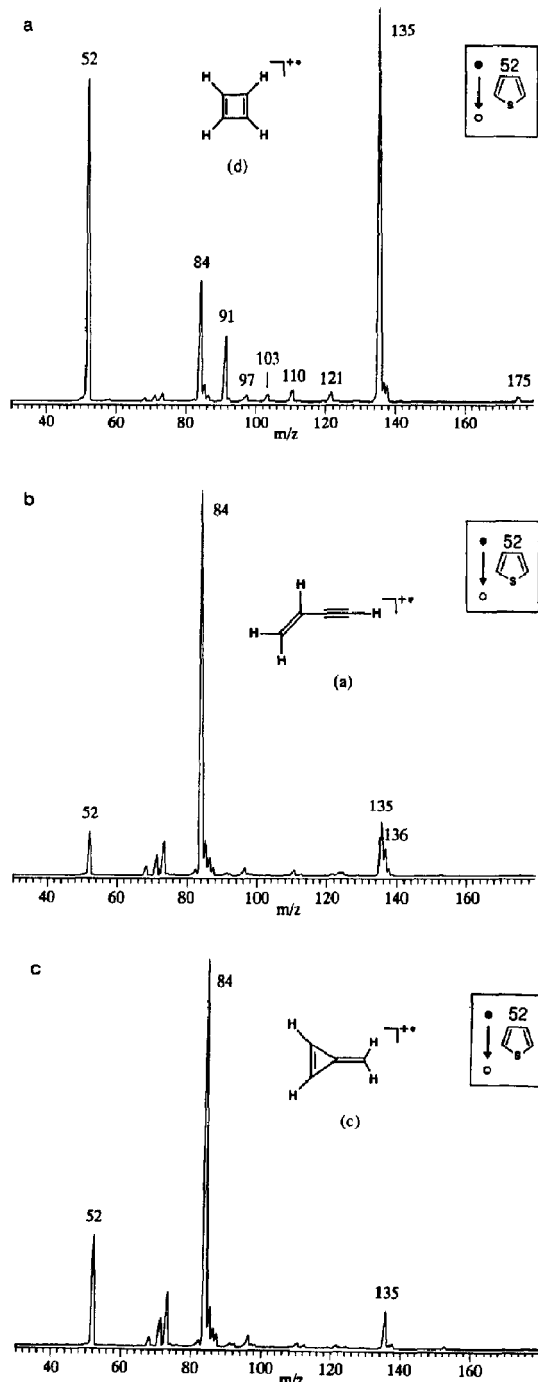
Figure 5. Product spectra of the ion-molecule reactions of (a) ion **d**, (b) ion **a**, and (c) ion **c** with neutral thiophene showing reaction products (m/z 135, 136, and 175) for **d** as opposed to primarily charge exchange product (m/z 84) for **a** and **c**. The spectrum for ion **b** is similar to that of **c**.
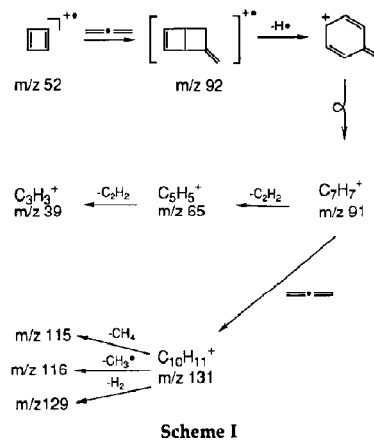
Sequential Product MS^3 Scans

It is possible to characterize the products of the ion-molecule reactions discussed above using the MS^3 capabilities of the pentaquadrupole instrument. Although MS/MS has been successfully used to probe ion or adduct structures following reactions in the ion source [5], relatively few studies have been performed by mass-selecting ions prior to reaction and subsequent CAD of the products. This method greatly simplifies interpretation of reaction pathways because, unlike studies employing reactions in the ion source, the precursor ion is known with certainty. Two of the MS^3 scans used here are the sequential product spectrum, symbolized in Table 2 as ● ⇒ ● → ○, and the reaction intermediate spectrum, ● → ○ → ●. In one series of experiments [Table 2, row (i)], the sequential product scan was performed on $C_4H_4^+$ ions that were mass-selected using Q1 (indicated by the first filled circle), made to undergo ion-molecule reactions with allene in Q2 to give products from among which a particular ion was mass-selected by Q3 (indicated by the second filled circle), and then dissociated by collisions with Ar in Q4. The products of CAD were then mass-analyzed (unfilled circle) using Q5 to record the spectrum. All three mass-analyzing quadrupoles are operated as mass filters in this experiment, Q1 and Q3 being set to select ions of particular mass-to-charge ratios while Q5 is scanned.

The sequential product scan was applied to examine reaction mechanisms and to investigate the structures of the products of ion-molecule reactions of the cyclobutadiene radial cation. This scan, performed by reaction of ion **d** with allene in Q2, mass selection of m/z 91 by Q3, and dissociation in Q4 by collision with argon while scanning Q5 to record the CAD products, produces a spectrum (Figure 6c) that shows an intense fragment ion at m/z 65 from loss of acetylene. Similar spectra (not shown) were observed for ions **a–c**. The $(C_7H_8^+)^*$ adduct itself fragments on formation, thus disallowing its mass selection for structural studies using MS^3 experiments. The low pressure used in the reaction quadrupoles (see "Experimental") results in a lack of stabilizing collisions and leads to decomposition of the incipient $(C_7H_8^+)^*$ adduct into $C_7H_7^+$ (m/z 91) + H· (Scheme I). Similar "condensation" behavior has been observed by Gross and co-workers for cycloadditions taking place in an ICR mass spectrometer in which low pressures are also used [29]. The tropylium ion is a likely candidate for ion m/z 91, but $C_7H_7^+$ isomers cannot be distinguished by low energy CAD experiments.

The initial reaction products of the $C_4H_4^+$ isomers most likely arise via cycloaddition, which has been demonstrated to be the predominant reaction between ionized alkenes and dienes [29b]. The pathway by which ion m/z 91 in Figure 1 is formed can be rationalized by an initial [2 + 2] cycloaddition of the

isomeric m/z 52 ions with allene to yield $C_7H_8^+$ (Scheme I).* This ion is produced with sufficient internal energy (223 kJ/mol for **d**) [25] to undergo rapid fragmentation by hydrogen atom loss to form the stable m/z 91 ion. Allene addition to **d** is exothermic by $\Delta H^0 = \Delta H_f^0$ (adduct) − ΔH_f^0(d) − ΔH_f^0 (allene) = −223 kJ/mol [22, 25]. H· loss to form the tropylium ion is also exothermic by ΔH_f^0 (tropylium) + ΔH_f^0 (H·) − ΔH_f^0 (adduct) = −139 kJ/mol [25]. In fact, all sixteen reported mass spectra of $C_7H_8^+$ molecules show the loss of a hydrogen atom as the most abundant fragment [39].

Figure 6a shows that the sequential product spectrum of the ion-molecule product m/z 131, $C_{10}H_{11}^+$, displays m/z 91 as the major fragment, along with ions at m/z 65, 103, 115, 116, and 129. Formation of m/z 131 can be rationalized via allene addition to m/z 91 ($C_7H_7^+$), as shown in Scheme I. Reversion of this

---

*The mechanistic rationalizations in the reaction schemes follow standard organic chemistry principles; see ref 38.

Scheme I

reaction then leads from m/z 131 to the major m/z 91 fragment. The ion-molecule product ion, m/z 131, can also lose molecular hydrogen, a methyl radical, or
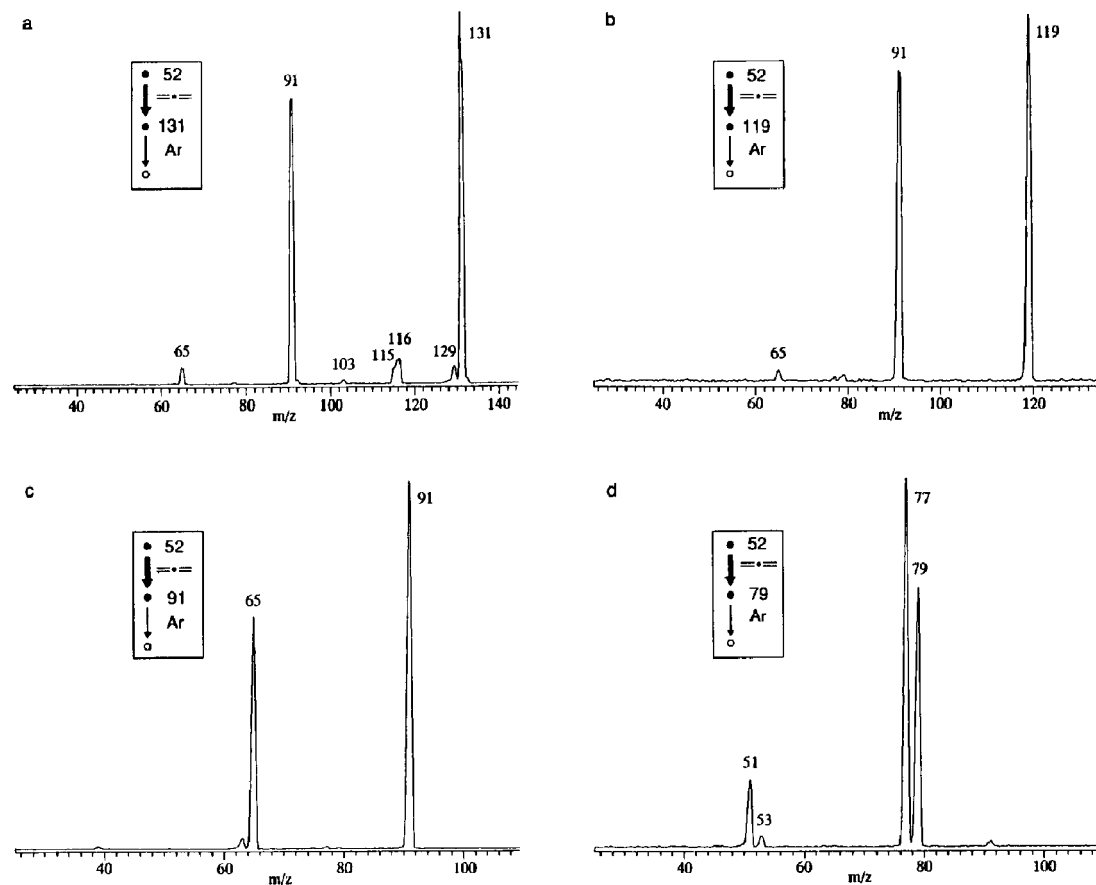
Figure 6. Sequential product spectra for the reaction of ion **d** with allene in Q2 followed by Q3 mass selection, in different experiments, of products 131, 119, 91, and 79 for subsequent dissociation using 10-eV collisions in Q4.

methane to yield m/z 129, 116, or 115, respectively. The m/z 129 fragment can dissociate further to m/z 103 by acetylene loss and hence yield m/z 77 by loss of a second molecule of acetylene. Scheme I summarizes the rationalizations made on the addition and fragmentation processes involved in the ion-molecule reaction of ion d with allene.

The m/z 119 and 79 ions observed in the $C_4H_4^{+\cdot}$ product spectra (Figure 1) are proposed to be formed by the cycloaddition of neutral allene to allene radical cations formed in Q2 by charge exchange with $C_4H_4^{+\cdot}$. Indeed, similar sequential product spectra to those shown in Figure 6b and 6d are obtained if, instead of ion d, ionized allene (m/z 40) is selected as the precursor for reaction with neutral allene. The m/z 119 and 79 products are therefore assigned as the allene trimer and dimer (each minus a hydrogen atom), respectively (Scheme II). Bowers et al. [35] have proved this pathway to m/z 79 formation by double resonance ICR studies. Our use of a four-centered intermediate for the initial $(C_6H_8^{+\cdot})^*$ adduct is based on deuterium-labeling data employed to explain ethylene loss [35]. The pathways that yield m/z 91 and 131 from allene self-condensation (Figure 2) are more complex. Based on the sequential product spectrum (Figure 6b), m/z 119 fragments by C_2H_4 loss, producing m/z 91. With the presence of neutral allene, this ion can form m/z 131 (Scheme II). The sequential product spectrum for m/z 79 (Figure 6d) shows extensive fragmentation of this ion by hydrogen loss to m/z 77 (very likely the phenyl cation) and further fragmentation to yield m/z 51, both processes being consistent with a protonated benzene structure for m/z 79 (Scheme II).

Reactions of ion d with isoprene were also examined using sequential product scans (Figure 7) and conclusions on reaction mechanisms are summarized in Scheme III. These spectra were acquired using isoprene in Q2 and mass-selecting, in turn, product ions m/z 173, 119, 117, and 105. In addition, the same experiments were done for m/z 103, 91, and 79 (not shown), again using CAD in Q4. The [4 + 2] Diels-Alder cycloaddition product ion (ion d + isoprene) of m/z 120 is not observed, suggesting that the expected addition product has enough internal energy to undergo fast fragmentation. Two expected fragment ions, m/z 119 and 105, expected from the cycloaddition product by loss of a hydrogen atom or a methyl radical, respectively, are observed. The sequential product spectrum for the sequence m/z 52 → m/z 119 → products (Figure 7b) shows fragmentation to give m/z 117, 104, 103, 91, and 79 by elimination of hydrogen, a methyl radical, methane, acetylene, and C_3H_4, respectively. It is also likely that ions m/z 117, 91, and 79 fragment further to m/z 115, 65, and 77 by loss of hydrogen, acetylene, and hydrogen, respectively. The spectrum for ion m/z 91 (not shown) reveals that this ion, like the products of reaction of $C_4H_4^{+\cdot}$ with allene, loses acetylene, forming m/z 65.
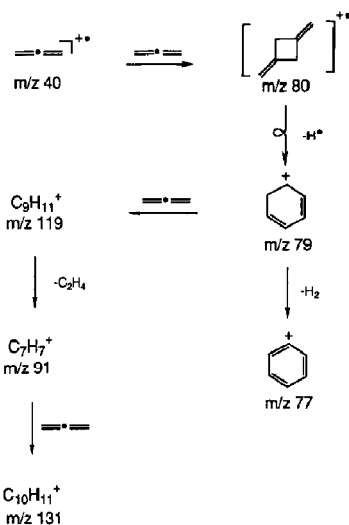
Scheme II

Again, the tropylium structure is tentatively assigned. Ion m/z 91 is also formed by acetylene loss from m/z 117 (Figure 7c), which also fragments to m/z 115 by hydrogen loss. Eliminations of hydrogen and acetylene from m/z 105 (Figure 7d) give ions of m/z 103 and 79, respectively, and further loss of acetylene and hydrogen yields m/z 77. Ion m/z 77 is the major fragment in the sequential product spectra of m/z 103 and 79. All of these processes are accommodated by the ion-molecule reactions and dissociations suggested in Scheme III.
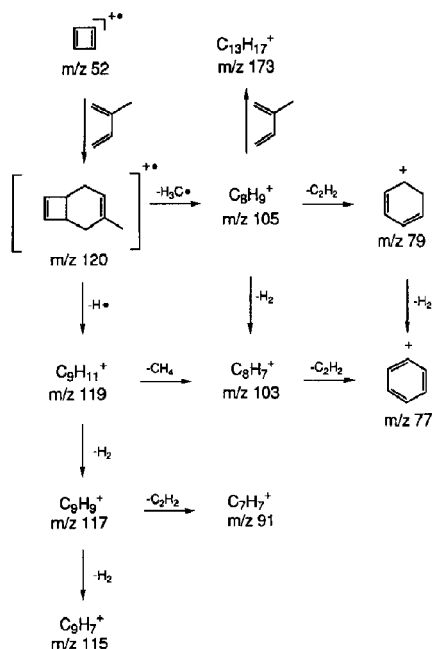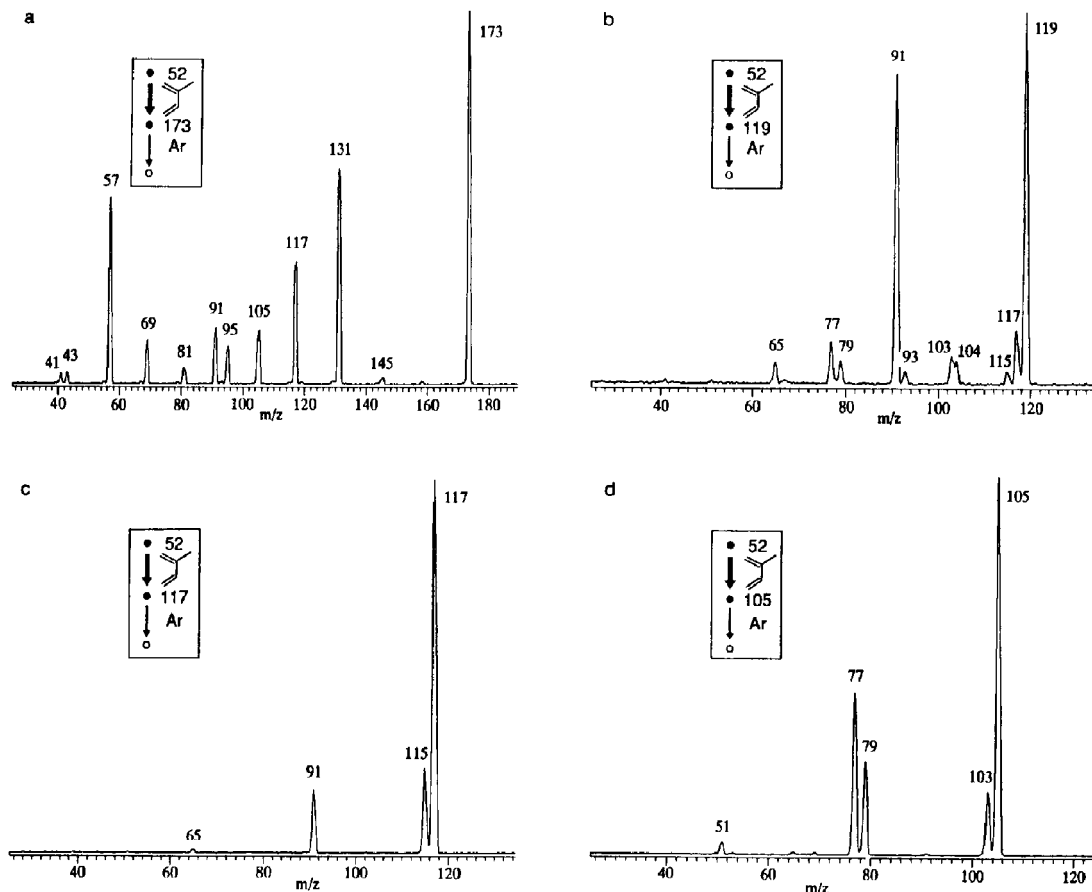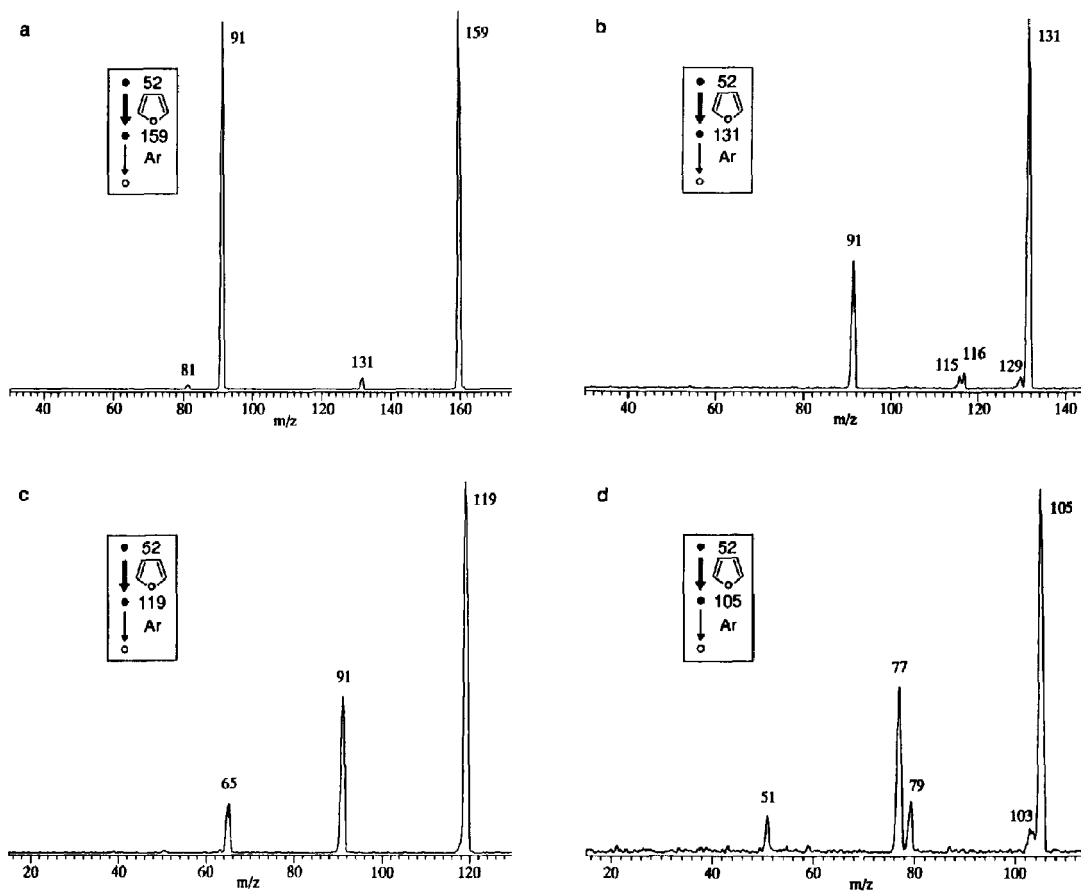

Scheme III

Figure 7. Sequential product spectra for the reaction of ion d with isoprene in Q2 followed by Q3 mass selection of products (a) m/z 173, (b) 119, (c) 117, and (d) 105, for subsequent dissociation using 10-eV collisions in Q4.
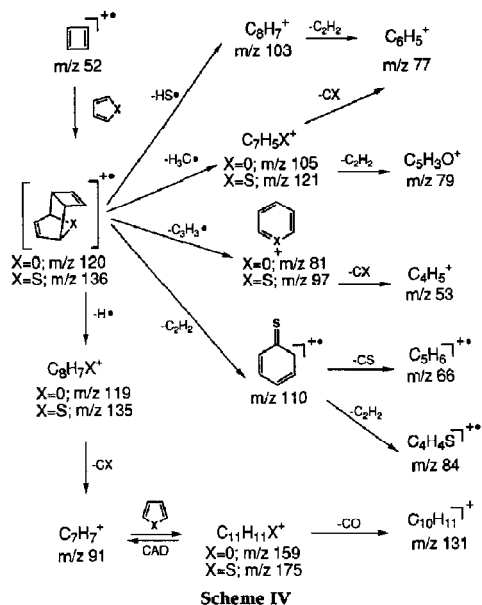
In addition to the [4 + 2] reaction and its products discussed above, products that arise from reactions that incorporate two neutral isoprene molecules are also seen. The product ion at m/z 173, observed in Figure 3a, is formally the result of addition of two isoprene molecules to m/z 52 accompanied by methyl radical elimination. Information on the nature of this ion was obtained by recording the sequential product spectrum m/z 52 → m/z 173 → products (Figure 7a). It is striking that this spectrum does not show ions of m/z 77 or 79; rather, the primary fragments at m/z 131 and m/z 117 are generated by loss of alkenes of 42 and 56 u. This suggests the presence of a cy-cloalkene unit in a nonaromatic structure analogous to the structure of the monoaddition product, m/z 120, shown in Scheme III.

The sequential product scans recording the fragmentation processes undergone by the products of reaction of $C_4H_4^{+}$ with furan (Figure 8) and thiophene (Figure 9) were also valuable in suggesting reaction mechanisms and fragmentation pathways (Scheme

IV). For the $C_4H_4^{+}$-furan reactions, the products at m/z 159, 131, 119, and 105 (and also 91, 81, and 65, data not shown) were mass-selected in turn prior to CAD. For the thiophene reactions, Q3 was set to select the products m/z 135, 121, 110, and 103 (and also 175, 97, and 91, for which data are not shown). The initial Diels-Alder cycloaddition adduct between $C_4H_4^{+}$ and furan or thiophene (Scheme IV) appears again to be unstable and to fragment by loss of a hydrogen atom to form m/z 119 (X = O) and 135 (X = S), by loss of a methyl radical to form m/z 105 (X = O) and 121 (X = S) or by loss of a C_3H_3 radical to form m/z 81 (X = O) and m/z 97 (X = S). The sulfur adduct, m/z 136, fragments by loss of acetylene or an HS radical to yield m/z 110 and 103 (Scheme IV). The greater stability of the hydrogen atom loss fragment from the sulfur adduct versus that from the oxygen adduct, reflected in the higher relative abundance of m/z 135 over m/z 119 (Figures 4a and 5a), is easily rationalized by the larger polarizability of the sulfur atom. The greater stability of the

thiophene adducts is also evident from the observation of an intact adduct with ion **a** in Figure 5b. The sequential product spectra for m/z 52 → m/z 119 and 135 (Figures 8c and 9a) show that the ion-molecule products readily lose CX to form ion m/z 91. The sequential product spectrum for this ion, m/z 91, generated from mass-selected $C_4H_4^{+\cdot}$, displays m/z 65 as the major fragment. The m/z 91 ion is proposed to react further with furan and thiophene (e.g., via electrophilic addition or a further cycloaddition) to form m/z 159 (X = O) and m/z 175 (X = S). This argument is supported by the sequential product spectra for m/z 159 (Figure 8a) and m/z 175, which show mainly the retroaddition fragment at m/z 91, formed by loss of 68 u (furan) and 84 u (thiophene), respectively. The observation of the m/z 131 fragment indicates that the product of addition to m/z 91 is not simply a loosely bound complex; that is, covalent bonds are formed. The m/z 131 ion seen in Figure 4a fragments (Figure 8b) to a similar set of ions, as does the m/z 131 product of reaction of ion **d**

with allene (Figure 6a). This indicates similar structures for both m/z 131 ions and supports the proposed fragmentation of m/z 159 (Figure 8a) to m/z 131 by loss of CO and not C_2H_4. Ions m/z 105 and 121 (Figure 9b) fragment by losing CX to yield m/z 77; the ion of m/z 105 also yields m/z 79 by loss of acetylene. Fragmentation via acetylene loss from m/z 103 yields m/z 77 (Figure 9d). These pathways are summarized in Scheme IV.

The $C_4H_4^{+\cdot}$-thiophene product is of special interest because m/z 110 is an odd-electron ion generated by acetylene elimination from the adduct. This rearrangement process occurs in the thiophene adduct but not in its oxygen analog, as is frequently the case for complex rearrangements [40]. Structural information was obtained by recording the sequential product spectrum, which reveals fragmentation mainly by CS (m/z 66) and acetylene (m/z 84) elimination (Figure 9c). The very low abundance of the fragment at m/z 77 corresponding to SH radical loss as well as the lack of some expected fragments for thiophenol—for in-

Figure 8. Sequential product spectra for the reaction of ion **d** with furan in Q2 followed by Q3 mass selection of products (a) m/z 159, (b) 131, (c) 119, and (d) 105, for subsequent dissociation using 10-eV collisions in Q4.
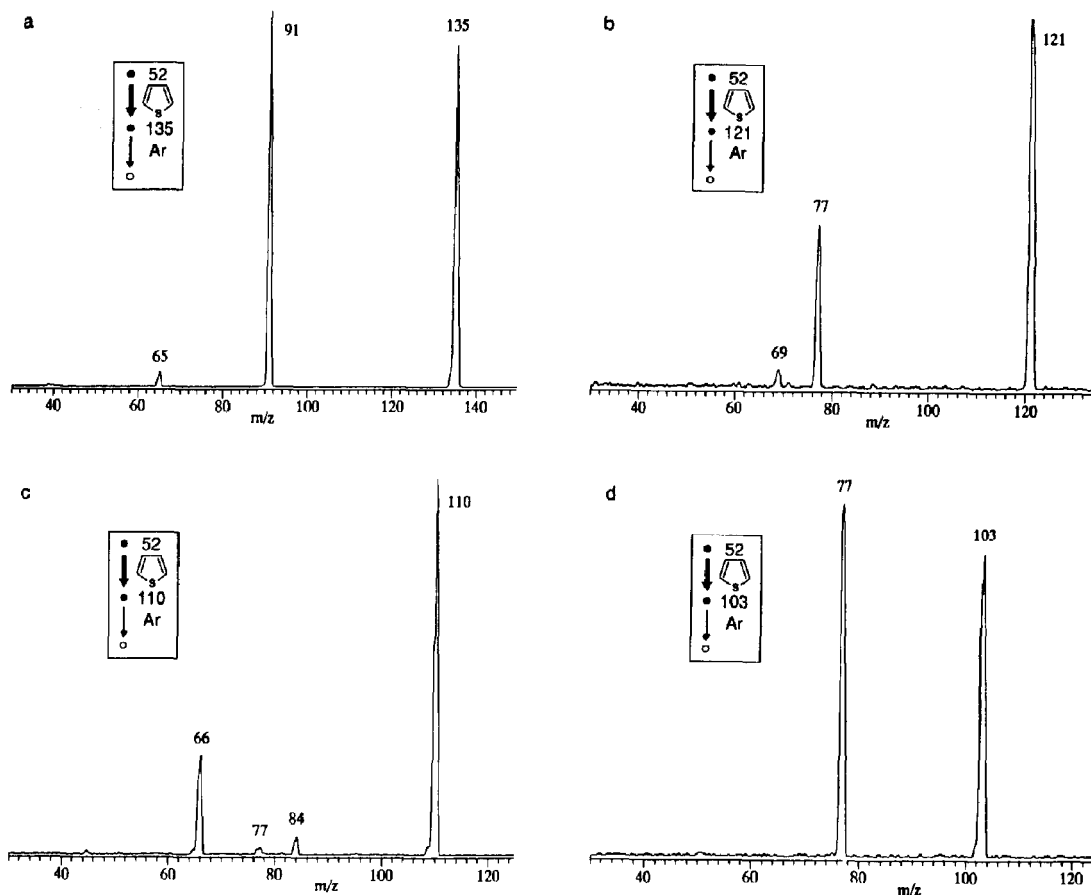
Figure 9. Sequential product spectra for the reaction of ion **d** with thiophene in Q2 followed by Q3 mass selection of products (a) m/z 135, (b) 121, (c) 110, and (d) 103 for subsequent dissociation using 10-eV collisions in Q4.

stance, m/z 65 and 69 [39]—rules out this structure m/z 110. The high abundance of the CS loss fragment suggests instead a thiocyclohexadiene or thiocycloheptatriene structure (Scheme IV). The fact that both m/z 97 and m/z 81 show very little fragmentation, displaying m/z 53 (loss of CX) as the only (for m/z 81) and major (for m/z 97) fragment in their sequential product spectra, suggests that they have very stable structures, and the pyrylium and thiopyrylium cations are likely candidates, respectively (Scheme IV).

Internal Energy Effects

A second type of sequential product scan experiment, row (ii) in Table 2, was used to examine the effects of changing ion internal energy prior to ion-molecule reactions; $C_4H_4^+$ was again selected using Q1, but collisions with an inert reagent, cyclohexane, occur in Q2 at 5 and 100 eV collision energies prior to ion-molecule reactions with allene in Q4. The prior colli-

sions are not used to change the nature of the ion because m/z 52 was mass-selected in both Q1 and Q3; instead, an opportunity was provided for collisional activation or deactivation. Q3 was then used to reselect m/z 52 prior to ion-molecule reaction with allene in Q4. The experiment was intended to confirm the absence of significant internal energy effects on the structural assignments made on the basis of ion-molecule reactivity. For the two m/z 52 isomers examined, those from precursors 1 and 4, the spectral changes produced were minor when 5-eV collisions were used in an attempt to deactivate any excited ion-molecule products. However, activating 100-eV collisions showed an effect that was slightly larger for the ion generated from precursor 1 than 4. The largest difference is observed for m/z 79, the product of allene addition to allene radical cation formed via charge exchange (Scheme II). The abundance of this ion changed from 69% to 108% relative to m/z 91 when prior activating collisions were employed, whereas for **d** the abundance changed only from 18%

$C_8H_7^+$ m/z 103 $\xrightarrow{-C_2H_2}$ $C_6H_5^+$ m/z 77

m/z 52

−HS•

−CX

$C_7H_5X^+$
−H₃C• X=0; m/z 105 $\xrightarrow{-C_2H_2}$ $C_5H_3O^+$ m/z 79
X=S; m/z 121

X=0; m/z 120
X=S; m/z 136

−C₃H₃•

X=0; m/z 81
X=S; m/z 97 $\xrightarrow{-CX}$ $C_4H_5^+$ m/z 53

−H•

−C₂H₂

$C_8H_7X^+$
X=0; m/z 119
X=S; m/z 135

m/z 110 $\xrightarrow{-CS}$ $C_5H_6^{+•}$ m/z 66

−C₂H₂

$C_4H_4S^{+•}$ m/z 84

−CX

$C_7H_7^+$ m/z 91 $\underset{CAD}{\rightleftharpoons}$ $C_{11}H_{11}X^+$ X=0; m/z 159 X=S; m/z 175 $\xrightarrow{-CO}$ $C_{10}H_{11}^+$ m/z 131

Scheme IV

to 24%. The result is accommodated by the fact that collisional excitation of ion a by 0.11 eV would make charge exchange with allene thermoneutral, thus increasing the charge exchange cross section. These experiments failed to produce evidence for internal energy effects that might compromise the structural conclusions based on the ion-molecule reactions.

Reaction Intermediate Scans

The output of the final MS^3 experiment, type (iii) Table 2, a reaction intermediate spectrum, is obtained by scanning Q3 while setting Q1 and Q5 to select particular ions. The reaction intermediate scans done in this study employed allene in both Q2 and Q4 under conditions that favored ion-molecule reactions in both regions. The resulting spectrum reveals the masses of all intermediates that connect the selected precursor and final product ions. The aim of this type of experiment was to confirm the pathways suggested by the sequential product MS^3 scans. Two isomers of $C_4H_4^+$, c and d, were chosen for examination of their reactions with allene to give particular ion-molecule products, namely, m/z 79, 91, and 131.

Figure 10a and d displays the ionic intermediates that connect ions c and d, respectively, and the product ion m/z 91 upon reaction with allene. These extremely simple spectra verify that the m/z 52 ion is the main precursor of m/z 91. The ions of m/z 40, 79, and 119 were proposed above to be the charge-exchanged allene radical cation and its reaction products with neutral allene (see Figure 2 and Scheme II). This is now supported by the observation in the reaction intermediate spectra (Figure 10b and e) of a large m/z

40 (ionized allene) contribution to formation of m/z 79, which is to be expected considering that dimerization of m/z 40 followed by fast hydrogen loss leads directly to m/z 79 (see Scheme II). The low abundance of m/z 40 and 79 in Figure 10a and d eliminates the possibility that allene ions are important in the mechanism of m/z 131 formation through m/z 91 (Scheme I), and their low intensity in the reaction intermediate spectra connecting m/z 52 and m/z 131 (Figure 10c and f) verifies directly that these ions do not contribute significantly to m/z 131 formation. Note, in particular, the direct evidence for the two-step addition of allene to generate m/z 131. The m/z 91 peak (the immediate fragment of $C_4H_4^+$ addition to allene) adds a further allene molecule to form m/z 131. The fact that m/z 52 itself occurs as an intermediate to m/z 131 allows the possibility of a one-step (termolecular) addition in Q4 of two allene molecules to $C_4H_4^+$. However, this result can be better interpreted as a result of multiple collisions, which are expected at the pressures employed in Q4.

The behavior of ions c and d in the reaction intermediate spectra is similar, but significant differences occur. These differences are similar in magnitude to those seen in the other types of spectra examined and are largely a reflection of the extent to which charge exchange occurs. The reaction intermediate spectra give some insight into the relative contribution of charge exchange products. The increase in relative intensity in Figure 10a and c of the ion at m/z 40 and m/z 79 over that in Figure 10d and f shows that the pathways to products m/z 91 and 131 through the charge exchange ion m/z 40 are of more importance for ion c, consistent with its higher ionization energy (Table 1).

Conclusion

It is relatively simple to distinguish the isomeric $C_4H_4^+$ ions on the basis of their ion-molecule reactions but difficult to do so by conventional CAD methods. This is both because of the milder conditions used to perform ion-molecule reactions and because bond-forming processes allow a greater variety of products than bond cleavages, especially in small hydrocarbon ions. The cyclobutadiene radical cation d is especially easy to distinguish by its unique reactions with each of the four reagent neutrals employed herein. In addition, the reagent allene was shown capable of distinguishing ion b, whereas reactions with thiophene distinguishes ion a. To determine the set of four $C_4H_4^+$ isomers one need simply apply the allene and thiophene reactions. A methodology is now available using instruments limited to low collision energies to distinguish these isomers by reactions with the reagent gases used herein. An expected application is examination of $C_4H_4^+$ isomeric content from other precursors by comparison to reactions of the precursors used here. On the basis of these characteristic ion-
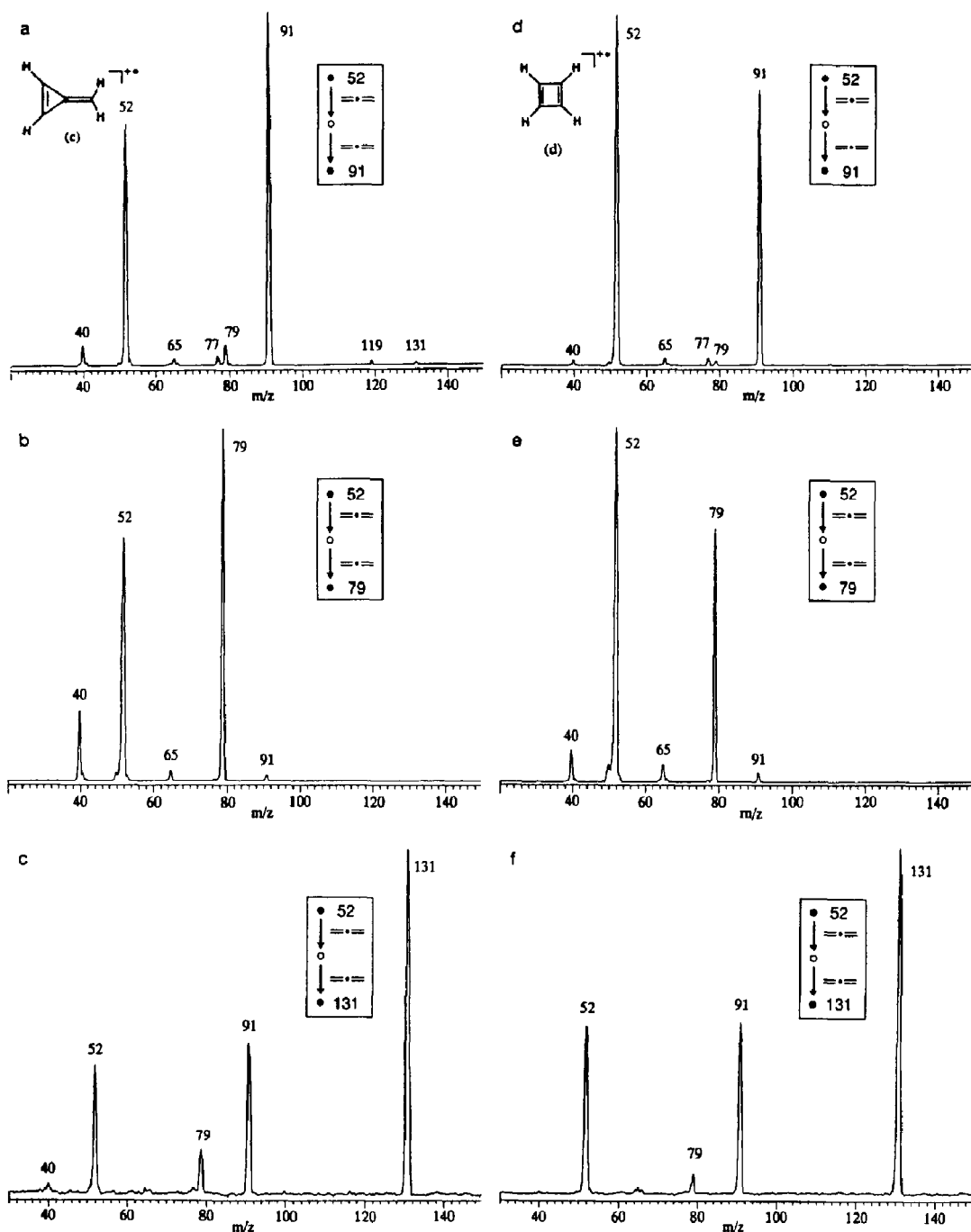
Figure 10. Reaction intermediate spectra for ions c (a–c) and d (d–f) using allene in both collision quadrupoles (Q2 and Q4) and scanning Q3 for all intermediates connecting m/z 52 (mass-selected in Q1) and m/z 91 for (a) and (d), 79 for (b) and (e), and 131 (mass-selected in Q5) for (c) and (f).

molecule reaction products, ion c was detected under the ion-molecule conditions used here as the major constituent of the $C_4H_4^+$ population formed by 70-eV EI of benzene (3). Also, negligible amounts of ion d were observed for precursors 1, 2, and 3. These results are in very good agreement with the conclusions of recent NRMS studies [22, 24].

The pentaquadrupole with its three mass analyzers and two reaction-collision cells allows the products of ion-molecule reactions to be explicitly characterized by a subsequent step of collision-activated dissociation. Such a sequence of processes is used to provide detailed information on the ion chemistry of ionized cyclobutadiene. In addition, ion-molecule reactions were performed in both reaction regions, and the nature of the ionic intermediates connecting specific reactants and products was elucidated through the reaction intermediate scan.

The highlights of the chemical findings are as follows: (1) Charge exchange and cycloaddition compete in the gas phase just as they do for radical cations in solution [30, 31]. Whenever the recombination energy of the $C_4H_4^+$ ion exceeds the ionization energy of the target, exothermic charge exchange is possible and makes a major contribution to the observed ion-molecule products. (2) The yields of $C_4H_4^+$ addition products to electron-rich dienes decrease in the order d > a, b > c. Ionized methylene cyclopropene exhibits a very low reactivity as dienophile in [4 + 2] cycloadditions; with this ion even endothermic charge exchange is more efficient than reaction. In sharp contrast, ionized cyclobutadiene is an excellent dienophile in the gas phase. Compounds that can produce ion d in situ, such as Carpenter's hydrocarbons [34], should show similar results in solution. (3) Ionized cyclobutadiene undergoes [2 + 2] cycloaddition with allene to give an adduct that fragments spontaneously to yield the $C_7H_7^+$ ion. Further allene addition is highly favorable, but it occurs without elimination of a neutral fragment. This closed-shell adduct is understandably more stable than the radical cation. (4) Ionized cyclobutadiene undergoes [4 + 2] cycloaddition with isoprene to yield an unstable adduct that eliminates a hydrogen atom or a methyl radical competitively. Both closed-shell ions undergo further isoprene addition to give stable products. (5) Reaction of ionized cyclobutadiene with furan and thiophene also yields unstable adducts that fragment by H˙, CH_3, and C_3H_3 elimination. The thiophene adduct undergoes acetylene elimination in a rearrangement reaction not shared by its oxygen analog. Addition of a second molecule of reagent to the formyl and thioformyl elimination fragments of the original ion-molecule reaction product also occurs.

Acknowledgments

References

1. (a) Gross, M. L.; Lin, P. H.; Franklin, S. J. Anal. Chem. 1972, 44, 974; (b) Ferrer-Correia, A. J. V.; Jennings, K. R.; Sen Sharma, D. K. Org. Mass Spectrom. 1976, 11, 876; (c) Budzikiewicz, H.; Busker, E. Tetrahedron 1980, 36, 255; (d) Keough, T. Anal. Chem. 1982, 54, 2540; (e) Staley, R. H.; Corderman, R. R.; Foster, M. S.; Beauchamp, J. L. J. Am. Chem. Soc. 1974, 96, 1260; (f) Bowers, M. T., Ed.; Gas Phase Ion Chemistry; Academic Press: Orlando, 1979, vol 2. (g) Harrison, A. G., Ed.; Chemical Ionization Mass Spectrometry; CRC Press: Boca Raton, FL, 1983; (h) Wittneben, D.; Brützmacher, H. F. Int. J. Mass Spectrom. Ion Proc. 1990, 100, 545.

2. Lias, S. G.; Liebman, J. F.; Levin, R. D. J. Phys. Chem. Ref. Data 1984, 13, 695.

3. (a) De Ruy, C. H.; Gronert, S.; Mullin, A.; Bierbaum, V. M. J. Am. Chem. Soc. 1990, 112, 8650; (b) Paulino, J. S.; Squires, R. R. J. Am. Chem. Soc. 1991, 113, 1845.

4. (a) Kenttämaa, H. I.; Cooks, R. G. J. Am. Chem. Soc. 1989, 111, 4122; (b) Kenttämaa, H. I.; Pachuta, R. R.; Rothwell, A. P.; Cooks, R. G. J. Am. Chem. Soc. 1989, 111, 1654; (c) Prome, D.; Prome, J. C.; Stahl, D. Org. Mass Spectrom. 1985, 8, 525; (d) Kinter, M. T.; Bursey, M. M. J. Am. Chem. Soc. 1986, 108, 1797; (e) Jalonen, J. J. Chem. Soc. Chem. Commun. 1985, 872; (f) Freeden, D. A.; Russell, D. H. J. Am. Chem. Soc. 1986, 108, 1860; (g) Gross, M. L. Adv. Mass Spectrom. 1989, 11a, 792; (h) Tabet, J. C.; Einhorn, J. Org. Mass Spectrom. 1985, 20, 310; (i) Bouchoux, G.; Hoppilliard, Y.; Jaudon, P.; Pechine, J. M. Rapid Commun. Mass Spectrom. 1987, 2, 20; (j) Eberlin, M. N.; Majumdar, T. K.; Cooks, R. G. J. Am. Chem. Soc. in press.

5. (a) Dymerski, P. P.; McLafferty, F. W. J. Am. Chem. Soc. 1976, 6070; (b) Lay, J. O.; Gross, M. L. J. Am. Chem. Soc. 1983, 105, 3445.

6. (a) Schwartz, J. C.; Schey, K. L.; Cooks, R. G. Int. J. Mass Spectrom. Ion Proc. 1990, 101, 1; (b) Morrison, J. D.; Stanney, D. A.; Tedder, J. Proc. 34th Am. Soc. Mass Spectrom. Conf. Mass Spectrom. Allied Topics, Cincinnati, 1986, p 222; (c) Beaugrand, G.; Devant, G.; Jaouen, D.; Rolando, C. H. Int. J. Mass Spectrom. Ion Proc. in press; (d) Mestdagh, H.; Morin, N.; Rolando, C. H.; Beaugrand, C.; De Maack, F. Proc. 34th Am. Soc. Mass Spectrom. Conf. Mass Spectrom. Allied Topics, Cincinnati, 1986, p 799.

7. Schwartz, J. C.; Wade, A. P.; Enke, C. G.; Cooks, R. G. Anal. Chem. 1990, 62, 1809.

8. Burinski, D. J.; Cooks, R. G.; Chess, E. K.; Gross, M. L. Anal. Chem. 1982, 54, 295.

9. Tomer, K. B.; Guenat, C. R.; Deterding, L. J. Anal. Chem. 1988, 60, 2232.

10. Louris, J. N.; Wright, L. G.; Cooks, R. G.; Schoen, A. G. Anal. Chem. 1985, 57, 2918.

11. Orlando, R.; Murphy, C.; Fenselau, C.; Hansen, G.; Cotter, R. J. Anal. Chem. 1990, 62, 125.

12. O'Lear, J. R.; Wright, L. G.; Louris, J. N.; Cooks, R. G. Org. Mass Spectrom. 1987, 22, 348.

13. Dolnikowski, G. C.; Health, T. G.; Watson, J. T.; Scrivens, J. H.; Rolando, C. H. J. Am. Soc. Mass Spectrom. 1990, 1, 481.